One- and Two-Dimensional Nuclear Magnetic Resonance Characterization of Poly(aspartic acid) Prepared by Thermal Polymerization of L-Aspartic Acid

Steven K. Wolk,* Graham Swift, Yi Hyon Paik, Kathryn M. Yocom, Rebecca L. Smith, and Ethan S. Simon

Rohm and Haas Company, 727 Norristown Road, Spring House, Pennsylvania 19477

Received June 8, 1994; Revised Manuscript Received September 12, 1994®

ABSTRACT: It is well-known that thermal treatment of aspartic acid produces poly(anhydroaspartic acid) (polysuccinimide), which can then be hydrolyzed to sodium polyaspartate. Both polysuccinimide and sodium polyaspartate have been analyzed by a variety of one- and two-dimensional NMR techniques. ^{1}H NMR indicates that sodium polyaspartate invariably contains a 3:1 ratio of β:α linkages, under a variety of synthesis and hydrolysis conditions. ^{13}C NMR and ^{1}H/^{13}C HMBC data show that the sequencing is random. Residual succinimide levels in sodium polyaspartate are detectable down to about 1% by ^{1}H NMR. COSY data of polysuccinimide and ^{1}H/^{15}N HMQC-TOCSY of polysuccinimide synthesized from 100% ^{15}N monomer indicate that phosphoric acid catalysis produces linear polymers, while uncatalyzed materials are branched.

Introduction

Amino acid homopolymers and their derivatives have long been known to exhibit interesting biochemical properties. Early work showed hormonal[1] and enzyme-like[2] activity, while more recent studies show inhibition of nephrotoxicity caused by antibiotics[3,4] and enhanced efficacy of *cis*-platinum complexes against carcinomas.[5]

The protein-like amide linkages found in poly(amino acids) offer, in principle, fully biodegradable polymers, which are desirable for many applications. Sodium polyaspartate has the additional characteristic of being a polycarboxylate polymer, which makes it attractive for applications requiring polycarboxylate functionality and no cumulative environmental effects. These uses include dispersants and scale inhibitors used in household laundry detergents and industrial waste water.

Sodium polyaspartate is commonly synthesized by thermal polymerization of aspartic acid monomer.[6,7] The initial product is poly(anhydroaspartic acid) (polysuccinimide), which must be hydrolyzed with caustic to obtain sodium polyaspartate. Because of the similar energetics of attacking either carbonyl, the product obtained is actually a mixture of two isomers, deemed α and β. The α subunit is the standard protein unit. The synthesis is summarized in Figure 1.

For characterizing the structure of polymers, NMR continues to be an extremely powerful tool. The majority of the effort in the literature has been applied toward DNA,[8] carbohydrates,[9,10] and proteins,[8] where a variety of multidimensional NMR experiments have been used to assign very crowded proton NMR spectra, as well as determine structural details such as conformation. In proteins, much larger molecules are now being studied with the advent of multinuclear three-dimensional experiments on proteins fully labeled with ^{13}C and ^{15}N.[11,12]

Though multidimensional NMR studies of synthetic polymers have been less prevalent due the similarity/overlap of backbone resonances,[13] some recent work has addressed characteristics such as average backbone conformation,[14] comonomer sequencing,[15–18] and stereochemical arrangement.[19–21] An amino acid homopolymer, in some respects, has characteristics of both proteins and synthetic polymers. Thus, two-dimen-

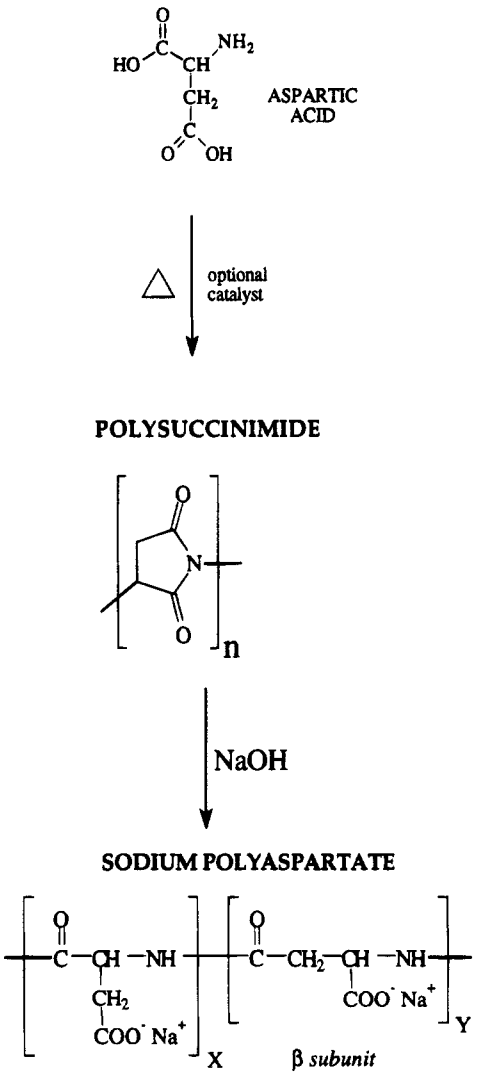

Figure 1. Synthetic route to sodium polyaspartate by thermal polymerization of aspartic acid.

® Abstract published in *Advance ACS Abstracts,* November 1, 1994.

0024-9297/94/2227-7613$04.50/0

sional NMR experiments typical of both biological and synthetic polymers proved useful in the present study.

Materials and Methods

Synthesis of Poly(anhydroaspartic acid) without an Acid Catalyst. A total of 104 g of L-aspartic acid was added to a glass beaker, and the beaker was placed in a preheated (270 °C) muffle furnace at atmospheric pressure. The reaction mixture was stirred with a spatula every 30 min. After 2 h, the reaction mixture turned from a white powder to a tan powder. After 8.5 h at 270 °C, the L-aspartic reaction mixture was removed from the muffle furnace. The yield was 75 g of tan powder. It was subsequently identified as poly(anhydroaspartic acid) with a M_w of 4400 and an M_n of 3570 using GPC.

Synthesis of Poly(anhydroaspartic acid) with 10% Phosphoric Acid as Catalyst. A total of 900 g of L-aspartic acid was mixed with 100 g of 85% phosphoric acid in a stainless steel pan, and the mixture was placed in a preheated (240 °C) muffle furnace at atmospheric pressure. The slightly wet white powder changed to a mixture of pink powder and yellow clumps after 1 h. After 1 h, the reaction mixture was ground to a fine tan powder with a mortar and pestle. The reaction mixture was stirred with a spatula every hour subsequently. After 8 h at 240 °C, the reaction mixture was removed from the muffle furnace. A total of 752 g of tan powder was obtained. It was subsequently identified as poly(anhydroaspartic acid). Syntheses of polymers with other levels of phosphoric acid were very similar.

Hydrolysis of Poly(anhydroaspartic acid) Prepared with 10% Phosphoric Acid as Catalyst. To a 1-L, four-neck flask equipped with a mechanical stirrer, thermocouple, condenser, pH probe, and inlet for additional base feed was charged 1054 g of deionized water. A total of 237 g of poly(anhydroaspartic acid) was then charged to the flask to form a mixture. The mixture was then heated to 90 °C. A dropwise feed of a 50 wt % solution of sodium hydroxide was then started. The feed was controlled using a Chem-Cadet (Cole-Parmer Instrument, Co., Chicago, IL) such that the feed would stop when the mixture reached a pH of 10.8. A total of 210 g of the 50% by weight sodium hydroxide solution was charged to reach a stable pH of 10.8. After the sodium hydroxide was charged, the mixture was held at 90 °C for 30 min and then cooled to room temperature. The mixture was then lyophilized until a dried sample of sodium polyaspartate (M_w = 8500, M_n = 5190) was obtained. Hydrolyses of other samples, catalyzed and uncatalyzed, were very similar.

Gel Permeation Chromatography. The weight-average molecular weights (M_w) and number-average molecular weights (M_n) were measured by aqueous gel permeation chromatography (GPC) relative to a M_w 4500 poly(acrylic acid) standard on a Progel TSK GMPWXL gel 30 cm × 7.8 mm column (Supelco, Inc., Bellefonte, PA), using a 0.1 M Na_2SO_4 mobile phase and a flow rate of 1.0 mL/min.

NMR Spectroscopy. All samples were analyzed on a Bruker AMX500 MHz NMR spectrometer.

For proton NMR experiments (one- and two-dimensional), about 5 mg of dried sample was added to a 5-mm NMR tube (Wilmad, Buena, NJ) already containing about 0.8 mL of solvent (99.96% D_2O (Cambridge Isotope Labs, Andover, MA) for sodium polyaspartate or 99.9% DMSO-d_6 (Cambridge Isotope Labs, Andover, MA) for polysuccinimide), and the mixture was immediately placed on a vortexer to obtain rapid dissolution. Samples for ^{13}C NMR and heteronuclear two-dimensional NMR were prepared the same way but were typically much more concentrated (up to hundreds of milligrams in some cases).

Proton NMR data were collected using a 5-mm dedicated proton probe or a 5-mm inverse detection probe. Typical acquisition parameters for the proton NMR spectra included a 3-μs (~40°) excitation pulse, 5300-Hz sweep width, 32K complex data set, 3.1-s acquisition time, and a 2-s recycle delay. Spectra in D_2O were referenced to TSP at 0 ppm (if used) or the water peak at 4.7 ppm. Spectra in DMSO-d_6 were referenced to the residual CD_3SOCD_2H peak at 2.49 ppm.

Carbon NMR data were collected using the decoupler channel of the 5-mm inverse detection probe tuned to the ^{13}C frequency. Typical acquisition parameters for the carbon NMR spectra included a 10-μs (~60°) excitation pulse, 27 778-Hz sweep width, 32K complex data set, 0.6-s acquisition time, and a 4-s recycle delay. Spectra in D_2O were referenced externally to a D_2O/dioxane sample. Spectra in DMSO-d_6 were referenced to the solvent peak at 39.5 ppm.

^{15}N NMR data were collected using the decoupler channel of the 5-mm inverse detection probe tuned to the ^{15}N frequency. Typical acquisition parameters for the nitrogen NMR spectra included a 20-μs (~60°) excitation pulse, 26 321-Hz sweep width, 16K complex data set, 0.31-s acquisition time, and a 1-μs recycle delay. (Scanning was set for maximum signal-to-noise at the expense of accurate quantitation). Spectra were referenced externally to $^{15}NH_4Cl$ in D_2O (0 ppm).

The COSY data were collected using the standard pulse sequence,[22] in magnitude mode using 90° pulses and a 1-s recycle delay. A total of 512 increments (32 scans per increment) was collected of 1024 complex points each, resulting in a 1024 × 1024 matrix after the two-dimensional Fourier transform. Prior to the transform, data were multiplied by a sine-bell apodization function.

Typical $^1H/^{13}C$ HMQC data were collected using the pulse sequence described by Bax, Griffey, and Hawkins.[23] The data were collected in magnitude mode, using a 1-s recycle delay, an evolution delay (1/2J) of 3.5 ms and GARP decoupling during acquisition. A total of 512 increments (128–256 scans per increment) was collected of 2048 complex points each, resulting in a 1024 × 1024 matrix after zero-filling and the two-dimensional Fourier transform. Prior to the transform, data were multiplied by a 45° phase-shifted sine-bell apodization function. Typical $^1H/^{13}C$ HMBC spectra were collected using the pulse sequence described by Bax and Summers.[24] The data were collected in magnitude mode, using a 1-s recycle delay, an evolution delay (1/2J) of 3.5 ms, a long-range evolution delay of 50–60 ms, and no decoupling during acquisition. A total of 512–1024 increments (32–256 scans per increment) was collected of 2048 complex points each, resulting in a 1024 × 1024 matrix after zero-filling (in the t_1 dimension only, if necessary) and the two-dimensional Fourier transform. Prior to the transform, data were multiplied by a 45° phase-shifted sine-bell apodization function.

The $^1H/^{15}N$ HMQC data were collected using the pulse sequence described by Bax, Griffey, and Hawkins (1983). The data were collected in magnitude mode, using a 1-s recycle delay, an evolution delay (1/2J) of 5.56 ms, and no decoupling during acquisition. A total of 256 increments (192 scans per increment) was collected of 1024 complex points each, resulting in a 1024 × 1024 matrix after zero-filling (in the t_1 dimension only) and the two-dimensional Fourier transform. Prior to the transform, data were multiplied by a 30° phase-shifted sine-bell apodization function. The $^1H/^{15}N$ HMQC-TOCSY data were collected using the pulse sequence described by Lerner and Bax.[25] The data were collected in phase-sensitive (TPPI)[26] mode, using a 1-s recycle delay, an evolution delay (1/2J) of 5.56 ms, an MLEV17 mixing pulse of about 60 ms, and no decoupling during acquisition. A total of 256 increments (256 scans per increment) was collected of 2048 complex points each, resulting in 1024 × 1024 matrix after zero-filling (in the t_1 dimension only) and the two-dimensional Fourier transform. Prior to the transform, data were multiplied by a 30° phase-shifted sine-bell apodization function.

Results and Discussion

Figure 2 shows a typical proton NMR spectrum of sodium polyaspartate in D_2O at pD 7.4. The methine proton is seen as two resonances at about 4.7 and 4.5 ppm. The methylene protons are observed as three resonances at about 2.8, 2.7, and 2.55 ppm. Any acid or amide protons would have exchanged with the bulk solvent (D_2O), and peaks for these species are not observed.

The ^{13}C NMR spectrum of sodium polyaspartate in D_2O at pH 7 is shown in Figure 3. The carbonyl carbons

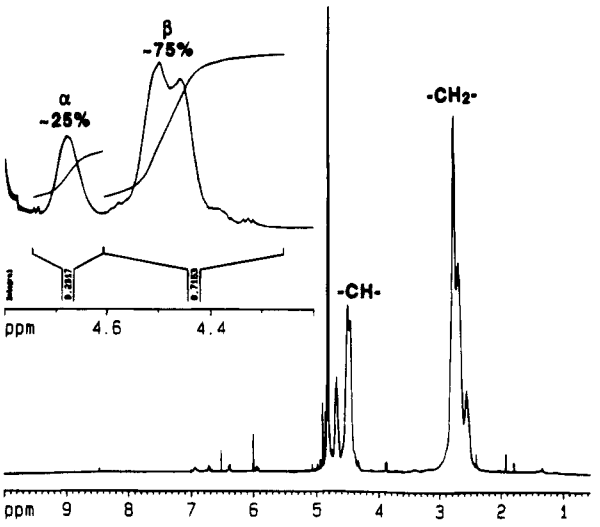

Figure 2. ^{1}H NMR spectrum of sodium polyaspartate in D_2O (pD 7.4). The inset shows an expansion of the methine region, showing resolution of the α and β methine protons.

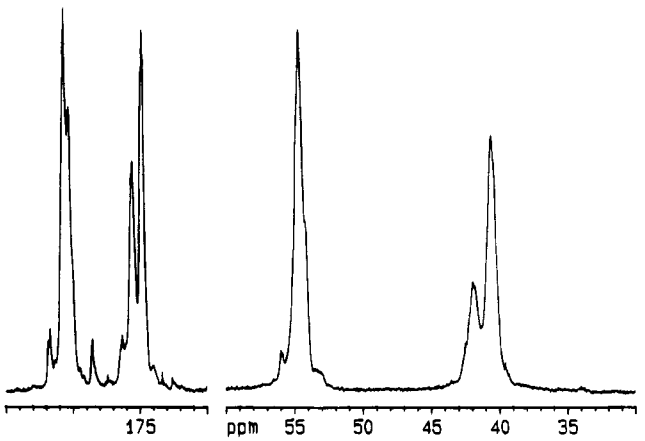

Figure 3. ^{13}C NMR spectrum of sodium polyaspartate in D_2O (pD 7.4).

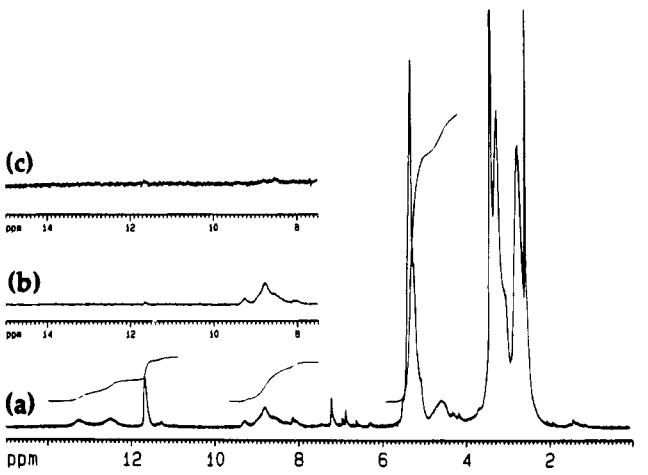

Figure 4. (a) ^{1}H NMR spectrum of polysuccinimide in DMSO-d_6. (b) Immediately after addition of 5 drops of D_2O. (c) 3 days after addition of D_2O.

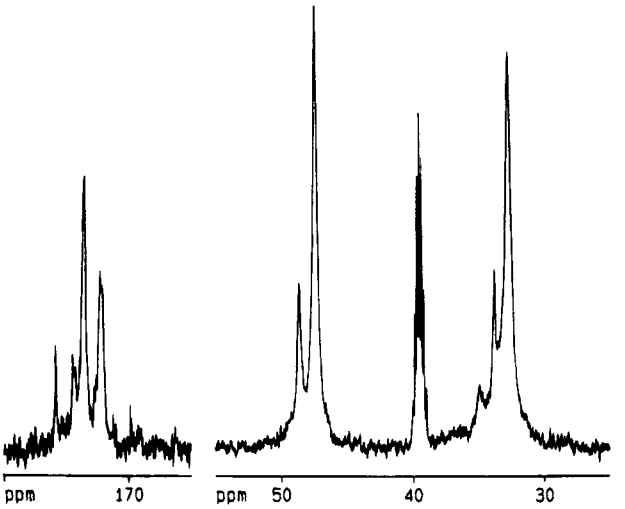

Figure 5. ^{13}C NMR spectrum of polysuccinimide in DMSO-d_6.

are observed in the 170–185 ppm region. There are two distinct groups of resonances, corresponding to the acid (downfield) and amide (upfield) carbonyls. These can be distinguished by a pH titration (data not shown), since the acid carbonyls are considerably more sensitive to changes in pH and the corresponding changes in chemical shift are larger. Also observed are the methine (51–57 ppm) and methylene (37–44 ppm) carbons.

The proton NMR spectrum of polysuccinimide in DMSO-d_6 is shown in Figure 4. The methine proton is observed as a large resonance at 5.2 ppm and a smaller peak at 4.6 ppm. The methylene protons are seen as two peaks of roughly equal intensity at about 3.3 and 2.6 ppm. A COSY spectrum (data not shown) shows that these methylene peaks are J-coupled, suggesting that they represent inequivalent methylene protons within one succinimide unit, as opposed to two structurally unique types of succinimide moieties. Partially superimposed on these peaks are the residual protonated DMSO peak ($CD_3(C{=}O)CD_2H$) at 2.49 ppm, to which the spectrum is referenced, and the residual water peak at about 3.5 ppm.

Two very broad resonances are observed at 12.48 and 13.22 ppm. Somewhat sharper resonances are observed at 11.60 and 11.22 ppm. These resonances are probably due to carboxylic acid and/or amine protons, which are most likely exchanging with the residual water as well as each other. The broad peaks between 8.0 and 9.5 ppm are consistent with amide protons of branched or ring-open sites. If these assignments are correct, then addition of a few drops of D_2O should cause the amine and acid protons to disappear almost immediately. (Due to their high rate of exchange with water, the site will be occupied by a deuterium atom most of the time, which is invisible in the proton NMR spectrum.) In contrast, the amide protons exchange more slowly, as is typically observed in proteins,[8] and these peaks will disappear slowly over the course of several days. This is exactly what is observed, as shown in parts b and c of Figure 4.

If it is assumed that the broad humps of near equal intensity 12.48 and 13.22 ppm are the two inequivalent carboxylic acid groups at the C-terminus of the polysuccinimide chain, an average degree of polymerization of 25 is obtained. This value is below that predicted from the GPC measurements, suggesting that other end groups may be present.

A typical ^{13}C NMR spectrum of polysuccinimide is shown in Figure 5. Two main carbonyl peaks are observed at 173 and 174 ppm, representing the two inequivalent carbonyls of the succinimide repeat unit. The repeat unit methylene and methine are observed at 32 and 47 ppm, respectively. Other small resonances in each of these regions are indicative of structural variations and/or end groups.

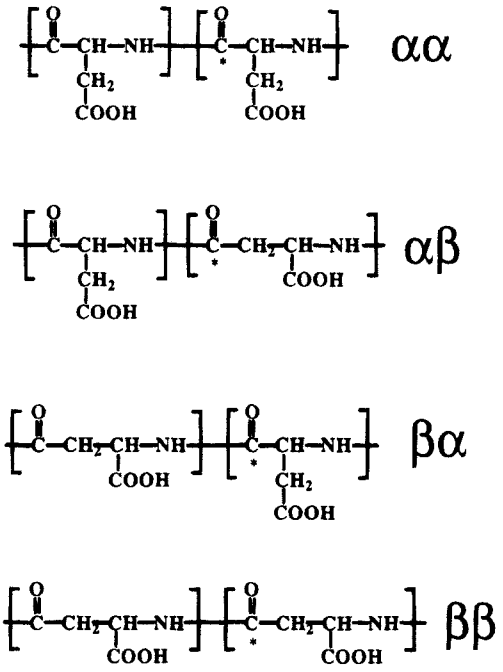

Figure 6. Structures of possible diad units in sodium polyaspartate.

α/β Ratios and Sequencing. The two methine proton resonances of sodium polyaspartate at 4.7 and 4.5 ppm (Figure 2) have been assigned to the β and α subunits, respectively.[27-29] At a field strength of 500 MHz, they are sufficiently resolved from each other (and the HDO resonance) to allow accurate integration; thus, the ratio can be trivially determined. The cross-peaks in the $^1H/^{13}C$ HMQC spectrum (data not shown) show that the methylene carbon peaks at 40.3 and 41.7 ppm can be assigned to the β and α methylenes. Regardless of synthesis conditions, it seems the hydrolysis of the polysuccinimide yields sodium polyaspartate that is about 75% β and 25% α. Clearly, ring opening leading to the β isomer is energetically favored over the α isomer. The α isomer is, of course, the type of linkage found in natural proteins.

Some information about the sequencing of the α and β units can be gained from the ^{13}C NMR spectrum and HMBC spectrum of sodium polyaspartate in D_2O at pH 7. In the carbonyl region of the ^{13}C spectrum (Figure 3), the amide carbonyls resolve into three major resonances. These peaks can be assigned in the HMBC spectrum, which shows coupling between protons and carbons two and three bonds apart.

As shown in Figure 6, three distinguishable diad units are possible; αα, αβ (βα), and ββ. In the αα diad, the central carbonyl carbon (marked by an asterisk in the figure) is within three bonds of two methine protons, both of which are α methines. Thus, in the HMBC spectrum, this carbonyl carbon should show cross-peaks only to α methine protons. Similarly, in the αβ or βα diad, the central carbonyl carbon is within three bonds of two methine protons: one α methine and one β methine. Therefore, in the HMBC spectrum, this carbonyl carbon should show cross-peaks to both α and β methine protons. By the same argument, the central carbonyl carbon of the ββ diad should show cross-peaks only to β methine protons.

The observed cross-peaks in the expansion of the HMBC spectrum (Figure 7) fit this description exactly, allowing assignment of the largest amide carbonyl (174.8 ppm) to ββ, the central peak (175.4 ppm) to αβ,

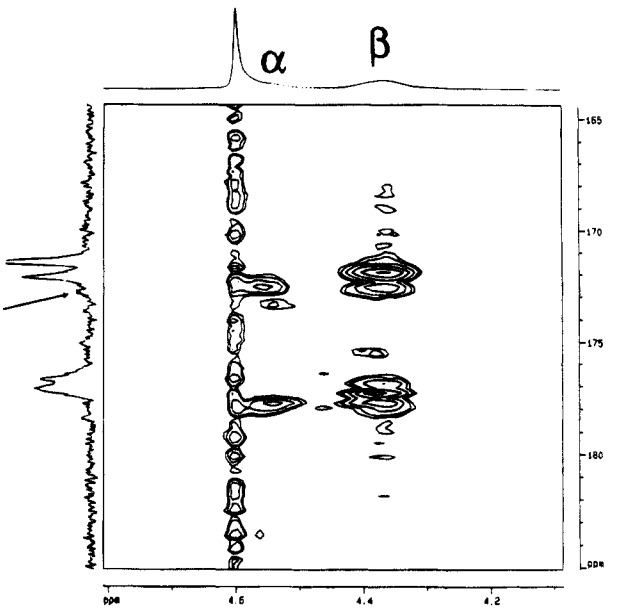

Figure 7. Expansion of the HMBC spectrum of sodium polyaspartate in D_2O (p*D* 7.4), showing the correlations between the methine protons and the carbonyl carbons.

and the smallest peak (176.3 ppm) to αα. These observed intensities match the expected intensities for random sequencing of a 75/25 polymer, as calculated from a simple statistical model.

Residual Succinimide Levels in Sodium Polyaspartate. As described above, ^1H NMR can easily distinguish sodium polyaspartate and polysuccinimide by the chemical shifts and peak distributions in the methine and methylene regions. It seems reasonable, therefore, that ^1H NMR can detect and quantitate the level of unhydrolyzed succinimide in sodium polyaspartate.

A control sample was thus prepared in which polysuccinimide was hydrolyzed with only 0.85 equiv of NaOH. The ^1H NMR spectrum of this sample at 60 °C in D_2O is shown in Figure 8. It should be noted that, at 60 °C, the water peak has shifted upfield to 4.45 ppm. When compared to the fully hydrolyzed material, it is clear that a new, broad resonance is observed at 3.15 ppm. This can be assigned to the most downfield of the two inequivalent methylene protons, based on consideration of the homopolymer spectra. (See above.) The sharp peaks overlapping the broader one and the additional peaks at 2.95 ppm in this region may indicate end groups or oligomers (which are possible byproducts of hydrolysis), though such peaks were not typically observed in fully hydrolyzed samples. In addition, new resonances are observed in the methine region at 4.9, 5.1, and 5.25 ppm. Again, this is consistent with the presence of succinimide residues, based on the homopolymer spectra.

To verify these assignments, COSY spectra of the 100% hydrolyzed and 85% hydrolyzed polysuccinimide were obtained, relevant expansions of which are shown in parts a and b of Figure 9, respectively. In the COSY spectrum of sodium polyaspartate (Figure 9a), the most downfield methine proton at 4.6 ppm shows coupling to the two most upfield methylene peaks. The cross-peaks between the methylene region and 4.4 ppm suggest that the second methine peak observed at room temperature is buried under the water peak at 4.45 ppm. This peak only shows coupling to the two larger methylene resonances. Another cross-peak reveals

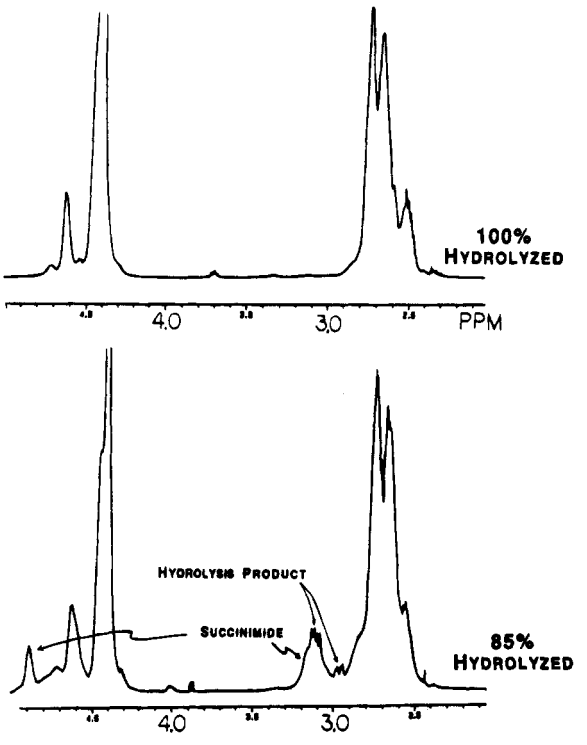

Figure 8. Comparison of the ^{1}H NMR spectra of 100% and 85% hydrolyzed polysuccinimide (sodium polyaspartate) in D_2O at 60 °C. (Sharp peaks, probably from low molecular weight byproducts, are seen in the 85% hydrolyzed sample, though this was not typically observed in fully hydrolyzed samples.)

coupling between a methine at 4.35 ppm and the smallest methylene peak at 2.5 ppm. As described above, the downfield methine can be assigned to the α subunits, and the upfield methine can be assigned to the β subunits. This, combined with the observed cross-peak pattern, suggests that the methylene peak at 2.75 ppm is solely from the β subunits, and the peaks at 2.65 and 2.5 ppm are from both α and β subunits.

The expansion of the COSY spectrum of the 85% hydrolyzed polysuccinimide (Figures 9b) shows most of the same cross-peaks, as expected. The new resonances at 3.1 ppm show a cross-peak ("A" in figure 9b) to 2.75 ppm. This is consistent with the succinimide methylene protons being inequivalent and *J*-coupled to each other, as observed in the homopolymer. (One is observed at 3.1 ppm, and the other is observed at 2.75 ppm, buried under the sodium polyaspartate methylene peaks.) These inequivalent methylene protons each show coupling (cross-peaks C) to the new methine resonances near 4.8 ppm, which is expected for the succinimide monomer unit. The small resonances at 5.1 and 5.25 ppm also show cross-peaks (D and E) to the succinimide methylenes and most likely represent low-frequency occurrences of the succinimide moiety such as end groups, or short oligomers. Cross-peak F probably correlates the byproduct peaks. It should be noted that the COSY data do not distinguish a copolymer from a mixture of homopolymers. In order to address the sequencing of the succinimide units, long-range coupling experiments including long-range COSY and HMBC were attempted and have thus far proved unsuccessful.

It follows that this analysis can be used to quantify the level of hydrolysis as a function of hydrolysis conditions. In principle, integration of the succinimide peak at 3.1 ppm (one methylene proton per unit) relative to the bulk methylene peak at 3.0–2.4 ppm (one succinimide methylene proton per unit plus two aspartic methylene protons per unit) yields the molar level of succinimide. Based on such integrations, the lower limit of detection of succinimide appears to be about 1%.

Phosphoric Acid Catalysis, Branching, and ^{15}N NMR. It has been reported[30] that aspartic acid thermally polymerized in the presence of phosphoric acid generates a polymer of increased molecular weight. It was recently been reported[31] that these polymers were completely biodegradable (sodium polyaspartate synthesized without an acid catalyst was found to be only 70% biodegradable[31]). It was, of course, of great interest to determine the structural basis of this difference in biodegradability. Figure 10 shows the ^{1}H NMR spectrum of the polysuccinimide form of the polymer as a function of phosphoric acid level. The key differences

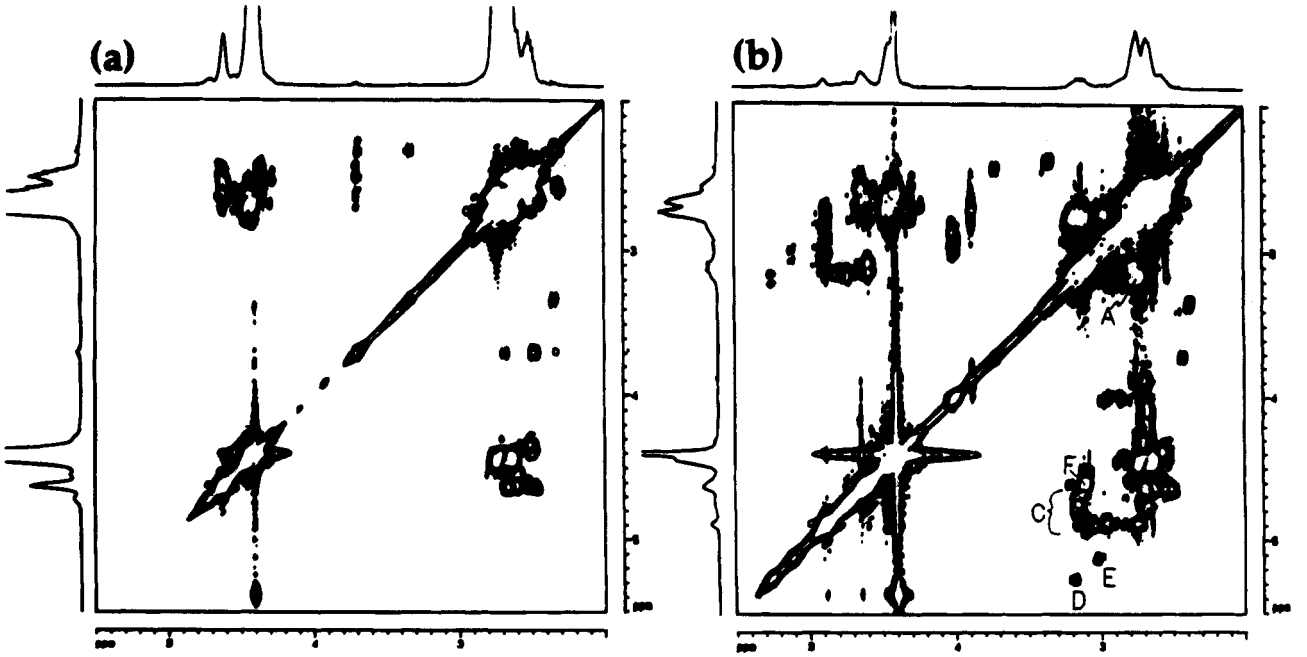

Figure 9. Expansion of the COSY spectrum of sodium polyaspartate in D_2O at 60 °C: (a) 100% hydrolyzed; (b) 85% hydrolyzed. The additional cross-peaks in the 85% hydrolyzed sample are consistent with the presence of succinimide residues.

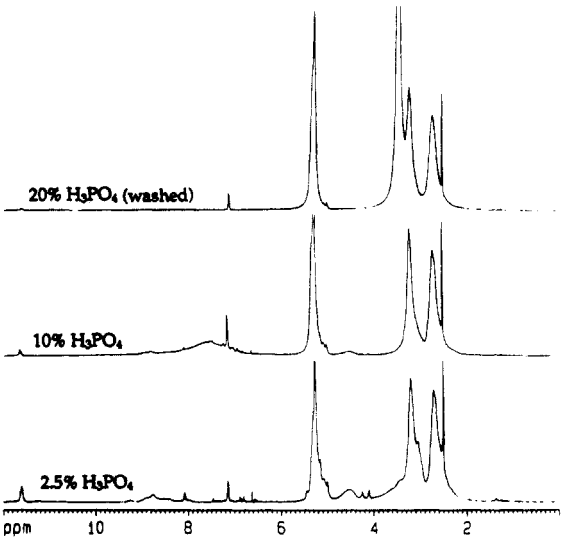

Figure 10. ^1H NMR spectrum of polysuccinimide in DMSO-d_6, as a function of phosphoric acid level used during synthesis. The 20% sample had been washed with water to remove the phosphoric acid prior to NMR analysis.

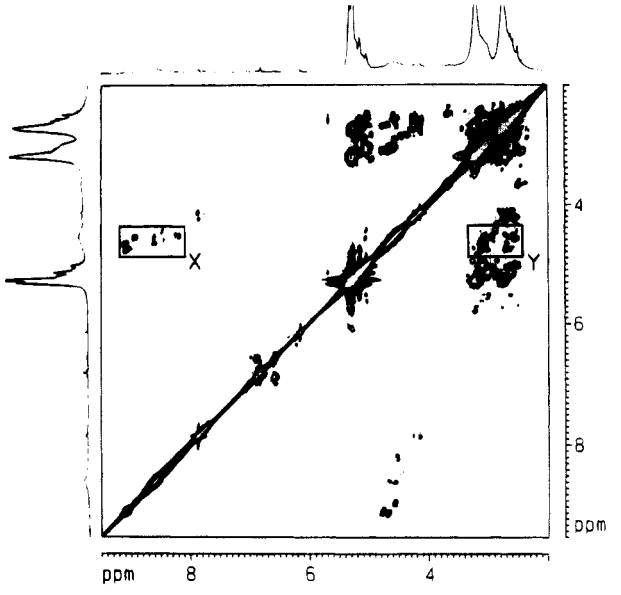

Figure 11. COSY spectrum of polysuccinimide (no catalyst) in DMSO-d_6.

in the spectrum are the intensity of amide protons (8–9.5 ppm) and the small methine peak at about 4.6 ppm, which get smaller in the 10% spectrum and essentially have disappeared from the 20% spectrum. In the 10% H_3PO_4 spectrum, the broad peak between 7 and 8 ppm is from the H_3PO_4 protons. In order to ensure that the disappearance of the amide protons was not due to a large increase in their rate of exchange, the 20% sample was first washed to remove the acid.

In order to definitively assign the structural entities which produce these resonances, a variety of NMR experiments were performed. Figure 11 shows the COSY spectrum of a typical uncatalyzed polysuccinimide. The cross-peaks in box X show that amide protons are J-coupled to the methines resolved at 4.6 ppm. The cross-peaks in box Y show that these same methines are also J-coupled to the partially resolved methylenes at about 3.1 and 2.6 ppm. Thus, the COSY data indicate that the structure shown in Figure 12 must be present at significantly higher concentrations in the uncatalyzed material. $^1H/^{13}C$ HMQC data (not shown) reveal that

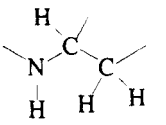

Figure 12. Structural entity present in uncatalyzed samples, as determined by two-dimensional NMR techniques.

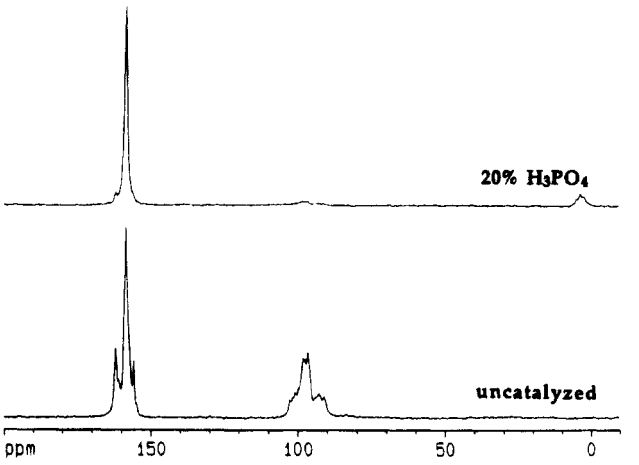

Figure 13. ^{15}N NMR spectra of 100% ^{15}N-polysuccinimide synthesized with no catalyst and with 20% phosphoric acid.

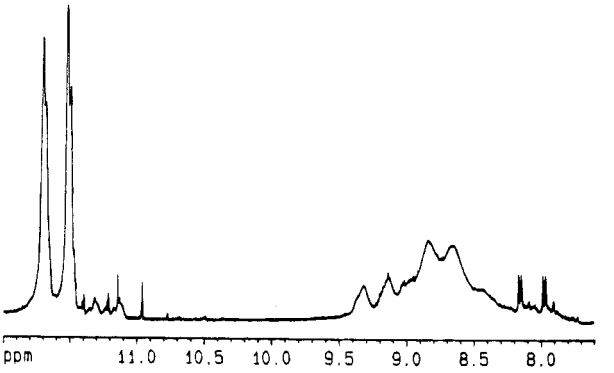

Figure 14. Expansion of the ^1H NMR spectrum of 100% ^{15}N-labeled polysuccinimide in DMSO-d_6.

the protons at 4.6 ppm are directly bound to the resolved methine carbon at 48.5 ppm.

In an attempt to obtain substantiating and/or additional evidence, a synthesis was undertaken using 100% ^{15}N labeled aspartic acid monomer. ^{15}N NMR spectra of the catalyzed and uncatalyzed material are shown in Figure 13. The sharp singlet at 158 ppm is undoubtedly from the standard succinimide repeat unit, which has no directly attached protons. The biggest difference between the spectra is clearly the intensity of the group of resonances ranging from 85 to 105 ppm. It is difficult to tell the multiplicity of these resonances due to overlap. In addition, the uncatalyzed spectrum shows several resonances nearly overlapping with the repeat unit peak. The spectrum of the catalyzed material shows additional small peaks near 0 ppm. One interesting ambiguity in the nitrogen NMR spectrum is the lack of definitive assignment of any of the resonances to the expected $-NH_2$ end group, which should be a triplet due to coupling to two protons. It is possible that the exchange rate of one or both of these protons is too rapid to observe the J-coupling.

Figure 14 shows an expansion of the ^1H NMR spectrum of the ^{15}N-labeled sample. The broad peaks between 7 and 9 ppm now appear as doublets ($J \sim 90$ Hz). This confirms that they are directly bound to

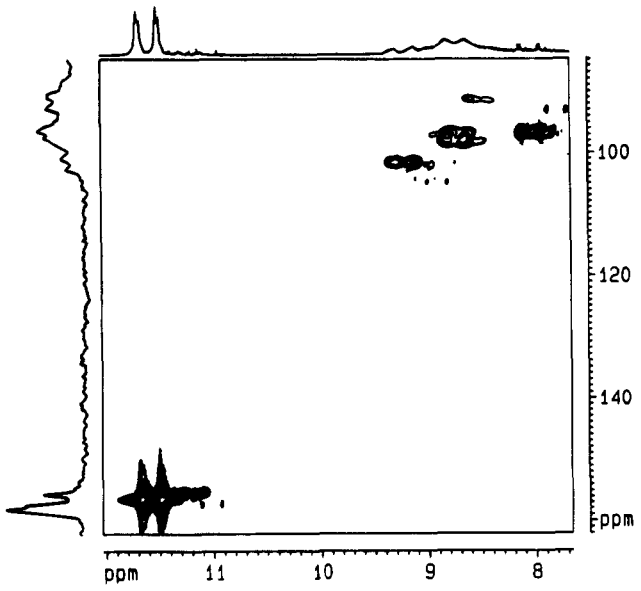

Figure 15. Expansion of the $^{1}H/^{15}N$ HMQC spectrum of 100% ^{15}N-polysuccinimide (uncatalyzed). No ^{15}N decoupling was applied during acquisition.

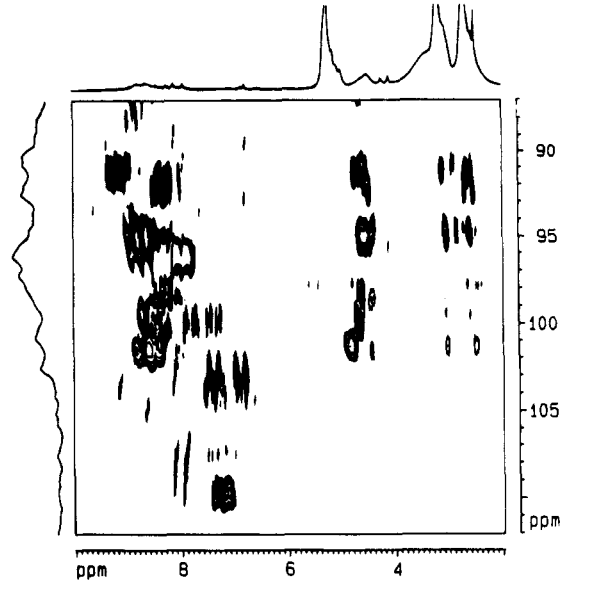

Figure 16. Expansion of the $^{1}H/^{15}N$ HMQC-TOCSY spectrum of 100% ^{15}N-polysuccinimide (uncatalyzed). No ^{15}N decoupling was applied during acquisition.

nitrogen, as would be expected for amide protons. The peak at 11.4 ppm also has become a doublet, suggesting that it is directly bound to a nitrogen.

To help assign these spectra, a $^{1}H/^{15}N$ HMQC spectrum was obtained, an expansion of which is shown in Figure 15. (In this experiment, no ^{15}N decoupling was applied during acquisition, which shows the multiplicity of the cross-peaks in the proton dimension.) The cross-peaks show that the peaks near 100 ppm in the ^{15}N spectrum are coupled to (and therefore directly attached to) the amide protons. As expected, the big peak at 158 ppm shows no cross-peaks, consistent with the succinimide repeat unit which has no attached protons. The nearly overlapping peaks (slightly shifted relative to the 1D spectrum shown in Figure 13, probably due to the slight change in temperature) show a cross-peak to the proton at 11.60 ppm. Clearly, these two peaks are a doublet. It is possible that one proton of the $-NH_2$ end group is hydrogen bound to one of the carbonyls of the final succinimide ring. This could result in two types of protons; one quickly exchanging and one slowly exchanging. This might result in the doublet appearance of the nitrogen peak. A second cross-peak is observed for a similar species barely detected in the ^{15}N spectrum, correlated to the peak at 11.22 ppm in the proton spectrum.

Figure 16 shows an expansion of the HMQC-TOCSY spectrum of the same sample. This spectrum shows that magnetization can be transferred from the nitrogen to the amide protons and then on to the methine protons and the methylene protons.

All the nitrogen and proton/nitrogen data fully corroborate the structure proposed above (Figure 12). The next step was clearly to determine what chemically reasonable structural entities in the polymer could contain this substructure. The only plausible structures seem to be the ring-open and branching sites, shown in Figure 17.

Unfortunately, the NMR results cannot unambiguously distinguish between these two structures. Other NMR experiments which may have distinguished the two were not successful. For example, a ROESY spectrum of the uncatalyzed sample was obtained, which might detect an ROE between two amide protons.

LINEAR FORM

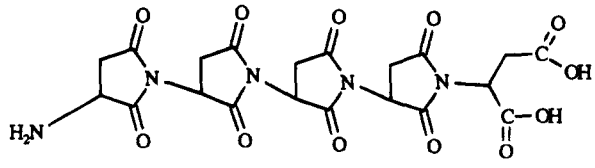

BRANCHED FORM

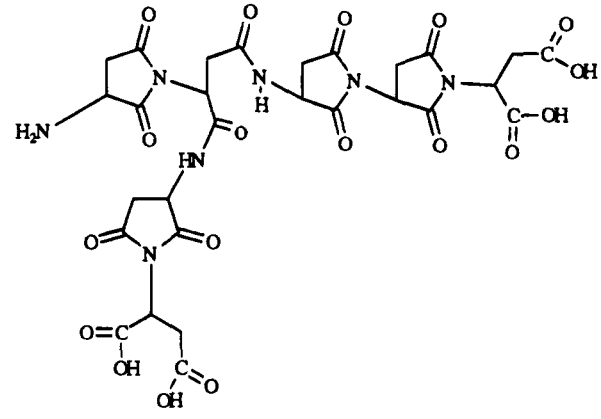

RING OPEN FORM

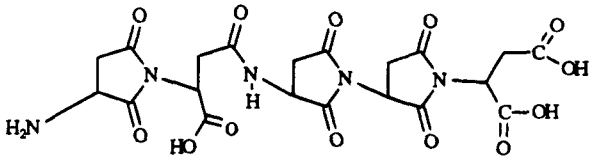

Figure 17. Proposed structures of polysuccinimide consistent with the spectroscopic data (assuming diacid and amine end groups, which may not be present in all chains).

Such spatial proximity might be detected for the branched structure but not for the ring-open structure.

In addition, an attempt was made to hydrolyze the catalyzed polysuccinimide at a 10% level, to see if the generated ring-open amide peaks would come to 4.6 ppm. Unfortunately, only a very tiny change was observed, certainly not consistent with 10% hydrolysis. The most likely explanation is that, due to the huge difference in water solubility of sodium polyaspartate and polysuccinimide, the chains which underwent initial hydrolysis solubilized and were hydrolyzed nearly completely in the water phase. The final result would then be 10% completely hydrolyzed chains and 90% unhydrolyzed chains. Thus, the chemical shift of randomly occurring ring-open sites could not be accurately determined by this experiment.

Though the branching and ring-open forms have not yet been distinguished, the biodegradation results of the hydrolyzed samples (i.e., sodium polyaspartate) show a significant difference;[30] samples which show the methine peak at 4.6 ppm degrade to about 70% completion, while samples which show no detectable methine peak at 4.6 ppm degrade completely (100%). Because ring-open sites are no longer distinguishable in the hydrolyzed polymer, this cannot explain the difference in biodegradation. Thus, branching sites must be present, unless there is some other structural difference(s) between the catalyzed and uncatalyzed polymers.

In summary, it seems that branching is the only reasonable explanation for the observed differences in biodegradation. It is indeed intuitively satisfying in that a branched polymer would provide a steric barrier to fitting the active site of a degradative enzyme designed/evolved for proteins. It would, of course, be useful to quantify the amount of branching by integration of the methine peak at 4.6 ppm. However, the integral probably represents contributions from both branching and ring-open forms, and it is likely that both are present at some level.

References and Notes

(1) Fox, S. W.; Wang, C. T. *Science* **1968**, *160*, 547.
(2) Dose, K. *Catalysis, Theor. Expt. Exobiol.* **1971**, *1*, 41.
(3) Williams, P. D.; Hottendorf, G. H. *Res. Commun. Chem. Pathol. Pharmacol.* **1985**, *47*, 317.
(4) Ramsammy, L. S.; Josepovitz, C.; Lane, B. P.; Kaloyanides, G. J. *J. Pharmacol. Exp. Ther.* **1989**, *250*, 149–153.
(5) Schechter, B.; Wilchek, M.; Arnon, R. *Int. J. Cancer* **1987**, *39*, 409–413.
(6) Katchalski, E. *Adv. Protein Chem.* **1951**, *6*, 123–185.
(7) Fox, S. W.; Harada, K.; Rohlfing, D. L. *Polyamino Acids, Polypeptides, and Proteins*; Stahmann, M., Ed.; University of Wisconsin Press: Madison, WI, 1962; pp 47–54.
(8) Wüthrich, K. *NMR of Proteins and Nucleic Acids*; John Wiley and Sons: New York, 1986.
(9) Morat, C.; Taravel, F. R.; Vignon, M. R. *Carbohydr. Res.* **1987**, *163*, 265–268.
(10) de Ward, P.; Leeflang, R. B.; Vliegenthart, J. F. G.; Vuister, G. W.; Kaptein, R. *J. Biomol. NMR* **1992**, *2*, 211–226.
(11) Ikura, M.; Kay, L. E.; Bax, A. *Biochemistry* **1990**, *29*, 4659–4667.
(12) Clore, G. M.; Bax, A.; Driscoll, P. C.; Wingfield, P. T.; Gronenborn, A. M. *Biochemistry* **1990**, *29*, 8172–8184.
(13) Bovey, F. A. *Chain Structure and Conformation of Macromolecules*; Academic Press: New York, 1982.
(14) Bovey, F. A.; Mirau, P. A. *Macromolecules* **1988**, *21*, 37–43.
(15) Bruch, M. D. *Macromolecules* **1988**, *21*, 2707–2713.
(16) Cheng, H. N.; Lee, G. H. *Macromolecules* **1988**, *21*, 3164.
(17) Beshah, K. *Macromolecules* **1992**, *25* (21), 5597–5600.
(18) Aoki, A.; Hayashi, T. *Macromolecules* **1992**, *25*, 155–160.
(19) Bruch, M. D.; Bovey, F. A.; Cais, R. E. *Macromolecules* **1984**, *17*, 2547–2551.
(20) Heffner, S. A.; Bovey, F. A.; Verge, L. A.; Mirau, P. A.; Tonelli, A. E. *Macromolecules* **1986**, *19*, 1628–1634.
(21) Miyatake, T.; Kawai, Y.; Seki, Y.; Kakugo, M.; Hikichi, K. *Polym. J.* **1989**, *21* (10), 809–814.
(22) Ernst, R. R.; Bodenhausen, G.; Wokaun, A. *Principles of Nuclear Magnetic Resonance in One and Two Dimensions*; Clarendon Press: Oxford, U.K., 1987.
(23) Bax, A.; Griffey, R. H.; Hawkins, B. L. *J. Magn. Reson.* **1983**, *55*, 301.
(24) Bax, A.; Summers, M. F. *J. Am. Chem. Soc.* **1986**, *108*, 2093–2094.
(25) Lerner, L.; Bax, A. *J. Magn. Reson.* **1986**, *69*, 375–380.
(26) Bodenhausen, G.; Kogler, H.; Ernst, R. R. *J. Magn. Reson.* **1984**, *58*, 370–388.
(27) Pivcova, H.; Saudek, V.; Drobnik, J.; Vlasak, J. *Biopolymers* **1981**, *20*, 1605–1614.
(28) Rao, V. S.; Lapointe, P.; McGregor, D. N. *Makromol. Chem.* **1993**, *194*, 1095–1104.
(29) Saudek, V.; Rypácek, F. *Int. J. Biol. Macromol.* **1988**, *10*, 277–281.
(30) Fox, S. W.; Harada, K. *Arch. Biochem. Biophys.* **1960**, *86*, 281–285.
(31) Yocom, K. M.; Freeman, M.; Paik, Y. H.; Swift, G.; Wolk, S. K., manuscript in preparation.